# DECAY FROM SUPERDEFORMED STATES IN THE MASS 190 REGION*

A. Lopez-Martens, F. Hannachi†, A. Korichi

CSNSM-IN2P3-CNRS, Bat. 104-108 Campus d'Orsay, 91405 Orsay, France

T. Dossing, B. Herskind

The Niels Bohr Institute, University of Copenhagen, Copenhagen, Denmark

T.L. Khoo and T. Lauritsen

Physics Division, Argonne National Laboratory, Argonne, IL 60439, USA

*(Received January 7, 2003)*

We report on the experimental results (past and present) concerning the decay from superdeformed states in the mass 190 region and on the two extreme theoretical approaches used to model the process. These two approaches can be combined into one using a chaoticity parameter. The possibilities of studying order-to-chaos properties of normally deformed states are discussed and illustrated by the analysis of the primary decay-out strength distribution in $^{194}$Hg.

PACS numbers: 21.10.–k, 23.20.–g, 23.20.Lv, 24.60.–k

## 1. Introduction

Super deformed (SD) states are populated in fusion-evaporation reactions at high spin. In 1% of the reactions, after the emission of cooling $\gamma$-cascades, the nucleus reaches the SD yrast line and follows it until it suddenly changes shape at low spin (8–10$\hbar$ in the mass 190 region). In doing so, the nucleus gains a considerable amount of deformation energy which it evacuates by emitting a series of $\gamma$-rays until it reaches the normally deformed (ND) yrast line which it in turn follows to the groundstate.

* Presented at the XXXVII Zakopane School of Physics "Trends in Nuclear Physics", Zakopane, Poland, September 3–10, 2002.

† Present address: CENBG/IN2P3, Gradignan, France.

The questions are: what does the decay-out spectrum look like, what are the excitation energy, spins and parity of SD states and what triggers the sudden shape change?

## 2. Experimental observations

Many experiments devoted to study of the decay from SD states have been carried out at Eurogam, Gammasphere and Euroball. It was possible to identify the four stages of the life of a SD nucleus [1]: first there is the feeding stage following the particle evaporation, with a statistical and collective component of weak unresolved transitions, then the well known picket fence like emission along the SD yrast line, after which comes the decay-out spectrum, also consisting of weak unresolved transitions which form a quasicontinuum, and finally the emission along the ND yrast line. From a quasicontinuum analysis, the average energy removed by the decay-out cascades can be extracted and consequently the average excitation energy of SD states at the point of decay. This turns out to be of the order of 3–4 MeV above yrast in the mass 190 region [1,2]. In a few cases, weak 1-step decay-out transitions (called links) can be observed in the high energy part of the decay spectrum and they give access to the absolute value of the spin and excitation energy of SD states. This is the case in $^{194}$Hg [3,4] and $^{194}$Pb [5,6] and the results are in good agreement with the quasicontinuum analysis results: the excitation energy of SD states at the point of decay is large. Also, there is a striking similarity between the decay-out spectrum and a spectrum of $\gamma$-rays following neutron capture at 7–8 MeV above yrast [7]. The general shape of the decay spectrum is well accounted for by statistical decay calculations if the effect of pairing on the ND level density is included [8]. Finally, a fluctuation analysis performed on the decay spectrum has shown that the decay is highly fragmented [9]: of the order of $10^4$ transitions are sampled by the $^{192}$Hg nucleus in the decay from SD states.

## 3. Decay mechanism

The decay occurs because of mixing with ND states: the SD wave function acquires a small amplitude, $\alpha^2$, at normal deformation. The SD state then has a partial width $\left(1-\alpha^2\right)\Gamma_{\mathrm{SD}}$ to decay to the next SD state and a partial width $\alpha^2\Gamma_{\mathrm{ND}}$ to decay to lower energy ND states. Even though the ND amplitude may be small, $\alpha^2 \times \Gamma_{\mathrm{ND}}$ can trigger the decay-out, especially since $\Gamma_{\mathrm{SD}}$ decreases when the SD nucleus looses spin whereas $\Gamma_{\mathrm{ND}}$ increases as the nucleus gains in excitation energy. If the coupling between ND and SD states is weak, the mixing will result in two states which are

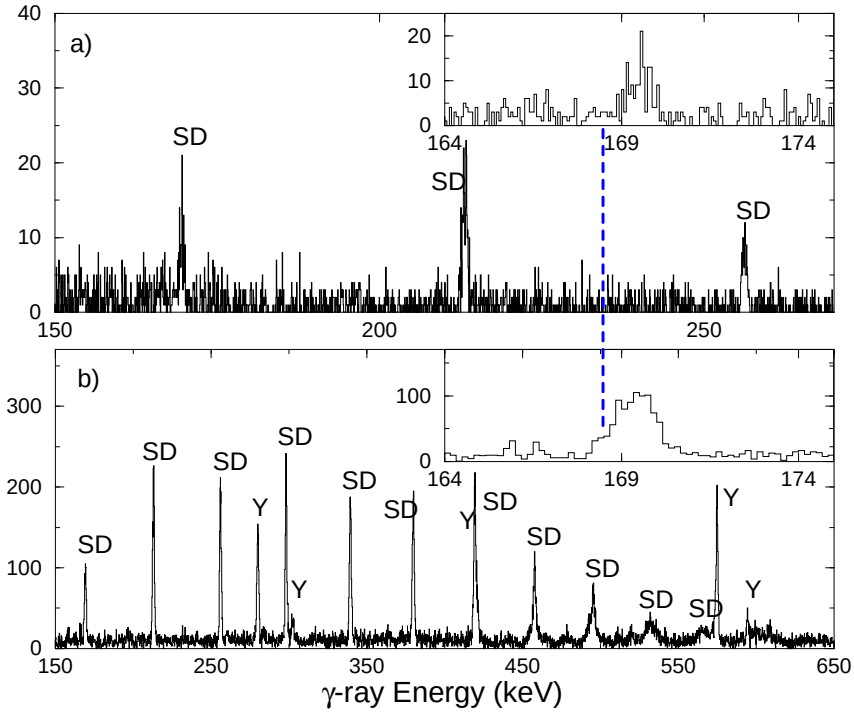


Fig. 1. (a) SD-gated spectrum of $\gamma$-rays detected in the LEPS detectors (b) SD-gated spectrum detected in the large volume detectors which had the best experimental resolution (7 out of 35). The SD symbols denote SD lines, the Y's denote ND yrast lines. The insets correspond to zooms around the 169 keV SD transition and the dotted line is to guide the eye between both spectra.

populated from the previous SD state proportionally to their SD amplitude squared: $\left(1-\alpha^2\right)$ for the predominantly SD state and $\alpha^2$ for the predominantly ND state. SD transitions populating SD decaying states should then effectively be doublets. This is clearly observed in the mass 130 [10] and 160 [11] regions. In the mass 190 region, however, the excitation energy of SD states is such that the average spacing between SD states and their closest ND neighbours is on average very small (tens of eV). This is too small to resolve, except maybe in the $^{194}$Pb case where the excitation energy of SD states at the point of decay is lower and where the density of ND states is reduced because $^{194}$Pb is a semi-magic nucleus at normal deformation.

To establish the mixing scenario in the mass 190 region, two experiments were performed at Yrastball and Gasp. In both cases, 5 LEPS (Low Energy Photon Spectrometers) were used because of their very good energy resolution at low energy (500–700 eV at 121 keV). This was essential if any splitting of the last SD transitions at 169 and 213 keV was to be observed.

A preliminary analysis of the Gasp data has revealed some strength to the left of the 169 keV transition in the spectrum of $\gamma$-rays detected in the LEPS detectors in coincidence with the SD band (panel (a) of Fig. 1). This excess strength is also visible in the spectrum of $\gamma$-rays detected in the large volume detectors (panel (b)) in Fig. 1): it seems indeed that the 169 keV transition has a shoulder towards low energies. The ratio of the intensities of the main SD $8^+ - 6^+$ peak and of its satellite yields a 15(5)% ND admixture into the $6^+$ SD state. The energy separation between the two peaks is 1.3(2) keV after interaction and 0.9(2) before interaction. The interaction strength is extracted to be 0.6(2) keV. The evidence for splitting is present but still weak. This is why the data is still being analysed in order to obtain more statistics in the relevant spectra.

The mixing can be modelled in different ways and there are two extremes:

- The ordered regime is well described by the Generator Coordinate Method [12–15]. Since mixing involves a deformation change, the collective states of the nucleus are described as linear combinations of HF+BCS $\alpha$-constrained solutions. These linear combinations are constructed in such a way as to minimize the expectation value of the Hamiltonian. The collective variable $\alpha$ is the mean mass quadrupole moment but it can include the mean octupole moment and the mean neutron and protong pair gaps. The GCM procedure mixes HF states and strongly depends on the pair gap and pairing vibrations. This collective model does not involve the coupling of the SD state with the multi-particle-hole states which lie in the first well at the same excitation energy and hence the probability to decay out is simply given by the ratio of the quadrupole transition probability to decay to lower energy ND collective states and to the next SD state.

- In the other extreme, the SD state is isolated by a potential energy barrier from a chaotic sea composed of compound ND states described by a random matrix [16,17]. The probability to decay out then depends on the ratio of ND and SD decay strengths and on the spreading of the tunnelling width among the ND states. The tunnelling width is given by the product of the SD state knocking frequency and the transmission coefficient. The action integral which gives the transmission coefficient is calculated along the least action path separating the SD and ND states. This involves hopping from one configuration of the nucleus to the next under the influence of the pairing residual interaction. The inertia of the system is, therefore, determined by the number of level crossings in the space of deformations and by the pairing gap and pairing vibrations.

The bridge between these two pictures can be made by introducing a chaoticity parameter [18]. In this picture, the SD state couples weakly only to specific ND states through the barrier (see Fig. 2). These states are called doorway states and they are equivalent to the HF+BCS states that the GCM procedure mixes with the SD state. The spectrum of ND states is described by a large matrix of size $N$. The matrix elements are random numbers selected from a Gaussian distribution centered around 0. There are two ways to introduce a degree of chaoticity in the spectrum: the off-diagonal elements of the random matrix can be scaled by $0 \leq \Delta \leq 1$ or there can be $1 \leq d_{\text{eff}} \leq N$ non vanishing elements per row (sparse matrix approach). If $\Delta = 0$, or $d_{\text{eff}} = 1$, the ND states do not mix and the SD state can only acquire an admixture of the nearest collective doorway state. If on the other hand, $\Delta = 1$ or $d_{\text{eff}} = N$, the doorway state has dissolved among all the neighbouring ND states and the SD state will acquire (via the fragmented strength of the doorway) an admixture of the closest complex neighbouring ND state.

The question that can be addressed is: what is $\Delta$ or $d_{\text{eff}}$ in the decay-out case?

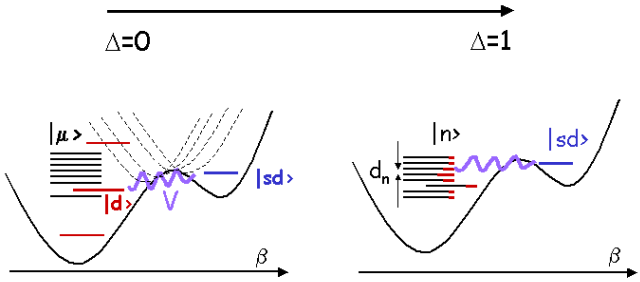


Fig. 2. Schematic representation of the two extreme coupling scenario between SD and ND states. On the left, the ordered case ($\Delta = 0$) where the SD state only couples to the closest collective ND state. On the right, the chaotic case ($\Delta = 1$) where the SD state couples to its closest ND neighbour via the fragmented strength of the collective ND states.

## 4. Order to chaos properties

The "chaoticity" of states has been addressed by a number of people in different regions of the (E,I) plane. The neutron resonances have been investigated [19], as well as near yrast levels in different nuclei [20]. A complete study of levels has been performed in $^{116}$Sn [21] and $^{26}$Al [22]. All these studies were done on the basis of level spacing statistics. The decay from SD states provides new regions of the (E,I) plane to study the chaoticity

of ND states: at low spin in the fission isomers, at moderate spins in the mass 190 region and at higher spins in the mass 150 region. The chaoticity of ND states with which the SD states mix can be studied by analysing the strength distribution of the transitions emitted in the first step of their decay. Jackson *et al.*, studied the properties of the $\gamma$-decay of 22 $1^-$ neutron capture resonances lying at 7.92 MeV in $^{196}$Pt [23]. The aim was to determine which distribution of primary strengths could account for the large intensity fluctuations observed in the $\gamma$-decay spectrum from one resonance to the next. The most likely distribution was found to be a $\chi^2$ distribution with $\nu = 1$ degree of freedom, often called a Porter–Thomas distribution [24]. This is a direct consequence of random matrix theory, and in particular, it reflects the properties of the Grand Orthogonal Ensemble (GOE) of matrices [25]. The particularity of the Porter–Thomas distribution is that unlike other $\chi^2$ distributions with higher degrees of freedom, it diverges towards low strengths, yet it also extends to very large strengths. This property gives rise to very strong strength fluctuations which could be the reason why single-step decay transitions are sometimes enhanced and can be observed experimentally. This is the case in $^{194}$Hg, for which strong high-energy links have been identified while in the neighbouring $^{192}$Hg, studied with similar statistics, no such lines could be observed (see Fig. 3).

In order to show that the enhancement of the strengths in $^{194}$Hg may be caused by Porter–Thomas fluctuations, a study of the primary strength distribution was performed. The aim was to determine which $\chi^2$ distribution of $\nu$ degrees of freedom and average strength $\theta$ could best fit the experimental strengths $\omega_i$ observed above the experimental strength threshold $\omega_{\rm low}$. The result for the most likely $\chi^2$ distribution is the following: $\nu = 1$ and $\theta$ is found to be nearly four times smaller than the experimental strength threshold [26]. The uncertainty on the number of degrees of freedom $\nu$ is very large because only the high-strength tail of the distribution is accessible experimentally and this is a strength domain for which there is not a pronounced difference between $\chi^2$ distributions. In other words, only the strongest 19 strengths are observed, whereas a fluctuation analysis in the same transition energy interval ($E_\gamma > 2.6$ MeV) tells us that there should be $\sim 600$. Nevertheless, we performed two simulations of 600 primary lines. Their strengths were sampled from the most likely strength distribution and their energies from an inverse level density formula. To these lines were added the experimental detector resolution, Compton and statistical feeding backgrounds and counting statistics. The spectra obtained above 2.6 MeV are shown in Fig. 3. They look very similar to the experimental decay spectra of $^{192}$Hg and $^{194}$Hg (top and bottom panels of Fig. 3, respectively) and in particular simulation #1, with strong lines at high energy, looks like the $^{194}$Hg spectrum whereas simulation #2 resembles the $^{192}$Hg case, with weak

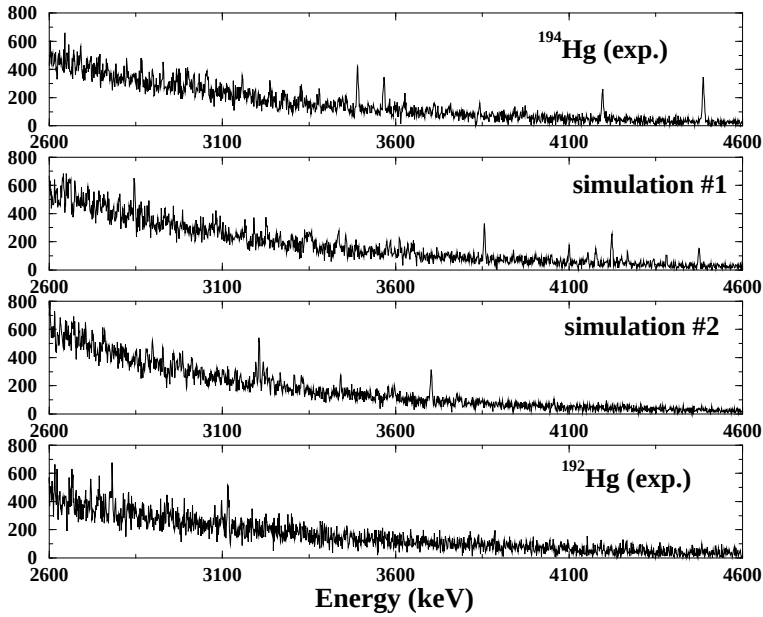


Fig. 3. Experimental decay spectra above transition energy 2.6 MeV in $^{192}$Hg and $^{194}$Hg (bottom and top panels) and 2 simulated spectra (see text for details).

and hence not so visible lines at high energy. So the chaotic nature of ND states with which the SD states mix through the barrier could explain why single-step links are observed in some nuclei and not in others.

Two important observations came out of the simulations. Firstly, the fact that a peak in the simulations stems very rarely from one line. This is specially true towards low energy since the inverse level density energy distribution yields many more lines at lower energies than at higher ones. The lines pile up one on top of the other and yield very broad and/or funny-shaped lines. This is what is called the *pandemonium* effect. Secondly, the effect of the counting statistics is non negligible. Given a set of simulated lines, if one changes the seed of the random number generator in order to produce different counting statistics, the shape and the intensity of the lines vary dramatically: some lines which are present and sharp in one spectrum disappear or become wide or even double in the other. This tells us that caution is needed when treating peaks at the very limit of the resolving power of the multidetectors and that setting a $3\sigma$ limit on the intensity of lines is the absolute minimum criterium to define a peak.

The problem in dealing with $\chi^2$ distributions is that it is not clear what $\nu \neq 1$ means. In order to overcome this problem, the chaoticity parameter introduced in Sec. 3 is used. Compound energy eigenstates of the nor-

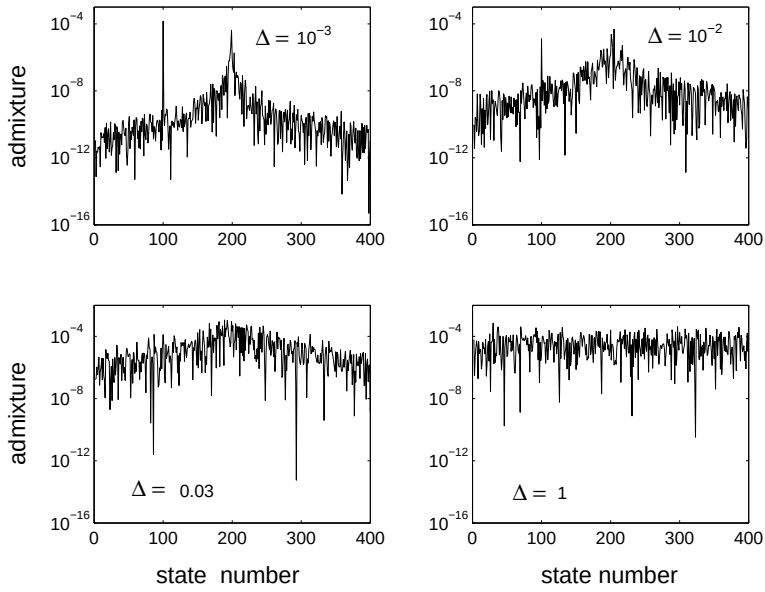


Fig. 4. Simulations of admixtures $|\langle\mu|S\rangle|^2$ of the basis states into the predominantly SD state for different values of the chaoticity parameter $\Delta$. The admixtures are normalised to the interaction strength $V$ and the average level spacing between ND states.

mally deformed spectrum are described by coupling the basis of $|\mu\rangle$ states with a Hamiltonian matrix selected from the Gaussian Orthogonal Ensemble. However, if part of the structure of the basis states is kept in the energy eigenstates, the off-diagonal matrix elements are reduced, and this is performed by scaling them with a common chaoticity parameter $\Delta$ ($0 \leq \Delta \leq 1$). The matrix is then diagonalised. After this procedure, the SD state $|sd\rangle$ is included in the middle of the spectrum together with its coupling $V$ to the doorway state $|d\rangle$ and one more diagonalisation is carried out. When $\Delta$ is equal to 1, the ND spectrum is fully mixed, the doorway state has dissolved among all the ND states and since the coupling $V$ is weak, one of the final states $|S\rangle$, which has a predominant SD component, will include many small admixtures of the original ND basis states $|\mu\rangle$. In the plot of the distribution of these admixtures into $|S\rangle$ for different values of $\Delta$ (Fig. 4), it is immediately clear what is meant by "chaos assisted tunnelling". For small values of $\Delta$, the admixture into $|S\rangle$ is mostly due to the doorway state (state 100) at an arbitrary value of $\sim 10^{-4}$ (the states in the middle of the spectrum, closest to the SD state, contribute also, but this is due to the energy denominator factor). When $\Delta = 1$, all the $N$ basis states will contribute on average with one admixture of that order: the admixture of

ND states into the SD state is $N$ times larger in the chaotic limit than in the ordered limit. To proceed further, the conjecture is that admixtures can be viewed as strengths: each basis state $|\mu\rangle$ is connected to one final state $|\mu'\rangle$ at lower energy. $N_{\rm s}$ simulations are carried out. For each simulation, $N_{\rm t}$ strengths are chosen. This corresponds to selecting a specific interval of transition energies, usually associated to the highest energies. Out of these $N_{\rm t}$, the $N_{\rm o}$ strongest (o for observed as in the experiment) are selected. The smallest of these $N_{\rm o}$ strength is then equivalent to the experimental strength threshold and all the strengths are normalised to it. For a given set of $\Delta$ and $N_{\rm t}$, 500 different GOE matrices of size $N = 400$ are diagonalised. The observational threshold is set to $N_{\rm o} = 19$, as in the $^{194}$Hg case. The average cumulative distribution is computed: the number of strengths observed as a function of strength averaged over the 500 simulations. The cumulative comparison is then defined as the fraction of simulations which display a larger $\chi^2$ deviation from the average cumulative distribution than the data. This is plotted in Fig. 5 as a function of $\Delta$ and $N_{\rm t}$. A data set is considered to be successful if it compares better than 25 % of the simulations. This condition is fulfilled when the total number of primary strengths is larger than 200 and when $\Delta$ is larger than 0.1. This determination of the relevant parameters is in agreement with the measurement of 600 primary lines in the 2.6–5 MeV transition energy range and with the result of the most likely $\chi^2$ distribution.

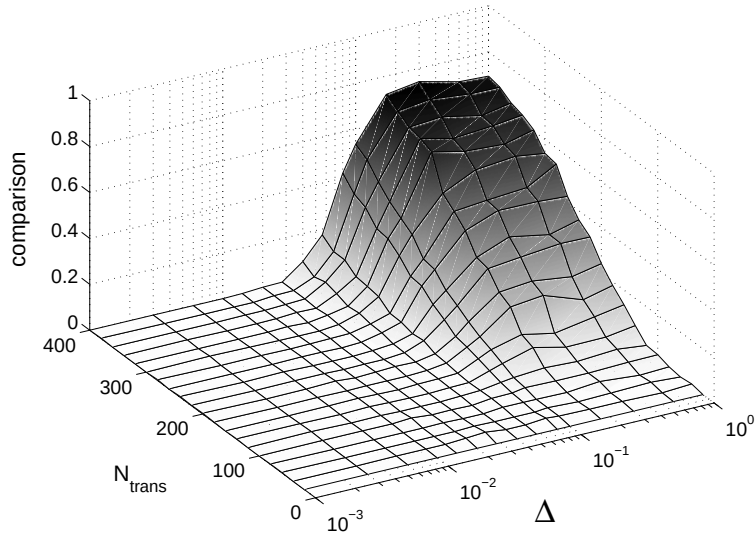


Fig. 5. Perspective plot of the comparison to simulated cumulative functions for the 19 visible decay-out transitions in $^{194}$Hg.

It appears, therefore, highly probable that the decay-out in $^{194}$Hg is a statistical process and that the ND states to which the SD states couple to at 4.2 MeV above yrast are compound states.

## 5. Conclusion

The decay-out of SD states provides new regions of the (E,I) for investigation of order to chaos properties of the nucleus. A new method based on a chaoticity parameter has been devised and its application to the decay from SD states in $^{194}$Hg shows that the decay in this nucleus is most probably chaotic. The analysis of the primary strengths using sparse matrices is in progress and currently, $^{194}$Pb and $^{236}$U are being investigated. Finally, the experimental difficulties associated with the identification of primary lines represent considerable limitations. The development of new, more powerful $\gamma$-arrays such as AGATA [27] and GRETA [28], based on the reconstruction of the photon trajectories in the germanium, will no doubt bring new prospects to this field of study.

The authors acknowledge that the experiment performed at LNL (Legnaro) with Gasp was supported by the following European Contracts: HPRI-CT-1999-00083 — V Framework Programme "Transnational Access to major Reaserch Infrastructures-Improving the Human Research Potential and Socio-Economic Knowledge Base" 01/11/00-31/10/03 and ERBFMGECT 980110 — IV Framework Programme TMR (Training and Mobility of Researchers) Access to Large Scale Facilities 01/04/98-30/04/01. This work was partially supported by the U.S. Department of Energy under contract W-31-109-ENG-38. The authors would like to thank J. Genevey (ISN, Grenoble) and G. Lo Bianco (University of Camerino) for lending their LEPS detectors.

## REFERENCES

[1] R.G. Henry *et al., Phys. Rev. Lett.* **73**, 777 (1994).

[2] T. Lauritsen *et al., Phys. Rev.* **C62**, 44316 (2000).

[3] T.L. Khoo *et al., Phys. Rev. Lett.* **76**, 1583 (1996).

[4] G. Hackman *et al., Phys. Rev. Lett.* **79**, 4100 (1997).

[5] A. Lopez-Martens *et al., Phys. Lett.* **B380**, 18 (1996).

[6] K. Hauschild *et al., Phys. Rev.* **C55**, 2819 (1997).

[7] T.L. Khoo, Proceedings from the Institute for Nuclear Theory on Tunneling in Complex Systems, Seattle, WA 1998, Ed. by Steven Tomsovic, World Scientific, Singapore, 1998, vol. 5, p. 229.

[8] T. Døssing *et al., Phys. Rev. Lett.* **75**, 1276 (1995).
[9] A. Lopez-Martens *et al., Phys. Rev. Lett.* **77**, 1707 (1996).
[10] D. Bazzacco *et al., Phys. Rev.* **C49**, R2281 (1994).
[11] J. Domscheit *et al., Nucl. Phys.* **A660**, 381 (1999).
[12] P. Bonche *et al., Nucl. Phys.* **A519**, 509 (1990).
[13] J. Meyer *et al., Nucl. Phys.* **A533**, 307 (1991).
[14] J. Meyer *et al., Nucl. Phys.* **A588**, 597 (1995).
[15] J. Libert, M. Girod, J.-P. Delaroche, *Phys. Rev.* **C60**, 054301 (1999).
[16] E. Vigezzi, R.A. Broglia, T. Døssing, *Phys. Lett.* **B249**, 163 (1990).
[17] Y. Shimizu *et al., Phys. Lett.* **B74**, 253 (1992).
[18] S. Aberg, *Phys. Rev. Lett.* **82**, 299 (1999).
[19] R. U. Haq, A. Pandey, O. Bohigas, *Phys. Rev. Lett.* **48**, 1086 (1982).
[20] J. Garrett *et al., Phys. Lett.* **B392**, 24 (1997).
[21] S. Raman *et al., Phys. Rev.* **C43**, 521 (1991).
[22] G. Mitchell *et al., Phys. Rev. Lett.* **61**, 1473 (1988).
[23] H. Jackson *et al., Phys. Rev. Lett.* **17**, 656 (1966).
[24] C. Porter and R. Thomas, *Phys. Rev.* **104**, 483 (1956).
[25] E. Wigner, *Proc. Cambridge Philos. Soc.* **47**, 790 (1951).
[26] A. Lopez-Martens *et al.*, *Nucl. Phys.* **A647**, 217 (1999).
[27] Agata Technical Proposal, J. Gerl *et al.*, `ftp://ftp.gsi.de/pub/agata/prop`.
[28] G.J. Schmid *et al., IEEE Trans. Nucl. Sci.* **3**, 975 (1997).